

Mechanism of fullerene hydrogenation by polyamines: *Ab initio* density functional calculationsEunja Kim,¹ Philippe F. Weck,² Savas Berber,^{3,*} and David Tománek⁴¹Department of Physics and Astronomy, University of Nevada Las Vegas, 4505 Maryland Parkway, Las Vegas, Nevada 89154, USA²Department of Chemistry, University of Nevada Las Vegas, 4505 Maryland Parkway, Las Vegas, Nevada 89154, USA³Physics Department, Gebze Institute of Technology, 41400 Gebze, Kocaeli, Turkey⁴Physics and Astronomy Department, Michigan State University, East Lansing, Michigan 48824-2320, USA

(Received 11 May 2008; published 9 September 2008)

We use *ab initio* density functional calculations to study the microscopic mechanism underlying the recently demonstrated hydrogenation of the C₆₀ fullerene by diethylenetriamine reagent. Our results indicate that the optimal monoaddition reaction is exothermic, involving an ≈ 0.5 eV high activation barrier associated with the simultaneous docking of the polyamine functional group and H transfer to C₆₀. Our calculated vibrational frequencies can be used to experimentally confirm the presence of hydroamination adducts as a necessary prerequisite for successful hydrogenation of C₆₀.

DOI: 10.1103/PhysRevB.78.113404

PACS number(s): 81.05.Tp, 68.55.ap, 73.61.Wp, 36.20.Hb

Chemical functionalization of well defined carbon nanostructures such as C₆₀ is an important direction to obtain a new class of molecules with intriguing properties. Among the many ways to chemisorb atomic hydrogen on C₆₀ and other *sp*² bonded nanocarbons, the recently introduced chemical reaction using high boiling polyamines appears as most promising.^{1–3} Alternative ways of hydrogenation using surfactants leave undesirable residue behind, and physical treatments such as ultrasonication^{4,5} often cause structural damage. In spite of the demonstrated efficiency of the polyamine-based hydrogenation, the microscopic mechanism underlying this reaction remains obscure.

In this Brief Report, we investigate the microscopic hydrogenation mechanism of C₆₀ by diethylenetriamine (DETA) reagent using *ab initio* density functional calculations. By exploring the DETA-C₆₀ potential-energy surface, we identify the structural changes and energetics along the optimal monoaddition reaction pathway. We find the hydrogenation to be exothermic, involving an ≈ 0.5 eV high activation barrier associated with the simultaneous docking of the functional group and H transfer to C₆₀. We also provide the vibrational spectrum of the hydroamination adduct to assist in the experimental confirmation of a successful hydrogen transfer to C₆₀.

Our total-energy calculations, as well as global and constrained structure optimization studies, have been performed using the density functional theory (DFT) within the local density approximation (LDA), utilizing first-principles pseudopotentials, as implemented in the DMOL3 (Refs. 6 and 7) and SIESTA (Ref. 8) software. In our DMOL3 (Ref. 6) calculations, we used the parametrization of Perdew and Wang⁹ for the exchange-correlation energy and a double numerical basis set, including polarization functions on all atoms (DNP). The DNP basis set corresponds to a double- ζ quality basis set with a *p*-type polarization function added to hydrogen and *d*-type polarization functions added to heavier atoms, and is comparable to 6–31G** Gaussian basis sets,¹⁰ providing a better accuracy at a similar basis set size.⁶ In the generation of the numerical basis sets, we used a global orbital cutoff of 3.7 Å. The energy tolerance in the self-consistent field calculations was set to 10^{–6} hartree. Optimized geometries were obtained without symmetry

constraints, using an energy convergence tolerance of 10^{–5} hartree and a gradient convergence of 2×10^{-3} hartree/Å. In our SIESTA (Ref. 8) calculations, we used an optimized double- ζ basis set with polarization orbitals,¹¹ the Perdew-Zunger¹² parametrization of the exchange-correlation functional, and norm-conserving *ab initio* pseudopotentials¹³ in their fully separable form.¹⁴ We used 0.01 eV/Å as a strict gradient convergence criterion during structure optimization.

The optimized geometries of DETA and C₆₀ reagents are shown in Fig. 1(a). In order to better understand the mechanism of hydrogen transfer from DETA to the C₆₀ molecule, we found it convenient to separate the DETA docking process from the hydrogen transfer between the docked polyamine and C₆₀. We considered different docking approaches, with the DETA axis normal or tangential to the C₆₀ surface. We found the latter, corresponding to DETA approaching with its end rather than its center, to provide the most favorable conditions for hydrogen transfer.

Our SIESTA results for the DETA docking process are shown in Fig. 1. To understand the energetics of the reaction, we performed a structure optimization of the DETA-C₆₀

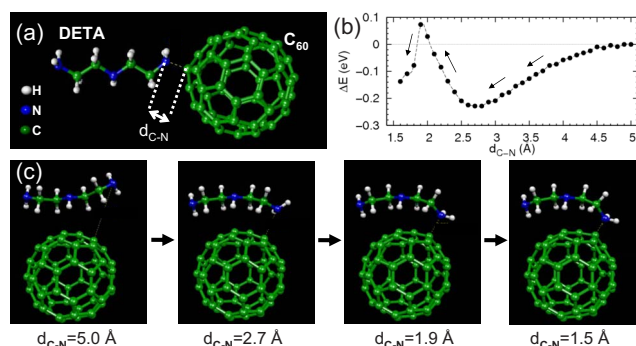


FIG. 1. (Color online) (a) Schematic of DETA docking to the C₆₀ molecule with the distance d_{C-N} between the terminal nitrogen of DETA and the closest C atom of the fullerene defining the reaction coordinate. (b) Total-energy change ΔE of the system as a function of d_{C-N} , taking the separated system as a reference. (c) Snapshots of the docking process, including the initial, transition, and final states.

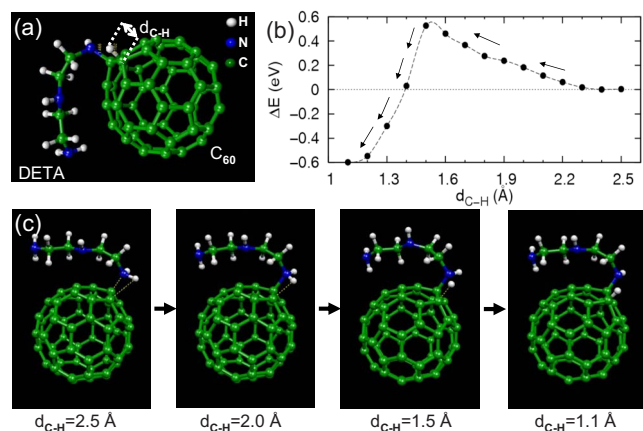


FIG. 2. (Color online) (a) Schematic of the hydrogen transfer from the docked DETA to the C_{60} molecule, with the distance d_{C-H} between the terminal hydrogen of DETA and the closest C atom of the fullerene defining the reaction coordinate. (b) Total-energy change ΔE of the system as a function of d_{C-H} , taking the initial-state system as a reference. (c) Snapshots of the hydrogen transfer process, including the initial, transition, and final state.

complex, constraining the distance between a terminal nitrogen atom in DETA and an atom of the C_{60} cage, as seen in Fig. 1(a). The total energy of the system as a function of the carbon-nitrogen distance d_{C-N} is depicted in Fig. 1(b). Our results indicate that DETA gains about 0.2 eV as it approaches from infinity and physisorbs near the fullerene. We note that physisorption with the DETA axis tangential to the surface, as seen in Fig. 1(c), is comparable in energy to a geometry with a radial orientation of the DETA molecule. Since in the latter case the overlap of DETA and C_{60} orbitals is less favorable for hydrogen transfer, we concentrate on the tangential adsorption geometry in the following. From the physisorbed state, DETA has to cross an activation barrier to chemisorb on the C_{60} cage at $d_{C-N} \approx 1.6$ Å, characteristic of a covalent bond. We found no ionic interactions between DETA and the C_{60} cage during the entire docking process since results of our Mulliken population analysis indicate absence of substantial charge transfer. Snapshots of the intermediate structures occurring during the docking process are shown in Fig. 1(c). The most striking change is the conformational change in the DETA molecule from its equilibrium linear geometry to a structure that adopts the curvature of the C_{60} cage upon adsorption.

To understand the transfer of a hydrogen atom from the chemisorbed DETA to the C_{60} cage, we performed a set of global optimizations starting with the docked structure, constraining the distance between a terminal hydrogen atom and a C atom in the cage, d_{C-H} , as seen in Fig. 2(a). The energetics of this hydrogen transfer reaction is depicted in Fig. 2(b). In view of the stability of the H-N bond, the initial energy investment of ≈ 0.5 eV to detach the H atom from DETA is rather small. The main reason for the reduced activation energy is the fact that bond breaking occurs simultaneously with the formation of a new bond in this concerted mechanism. The net energy gain during this exothermic reaction amounts to 0.6 eV. Following a simple Redhead's analysis of the migration temperature on solid surfaces,¹⁵ we estimate

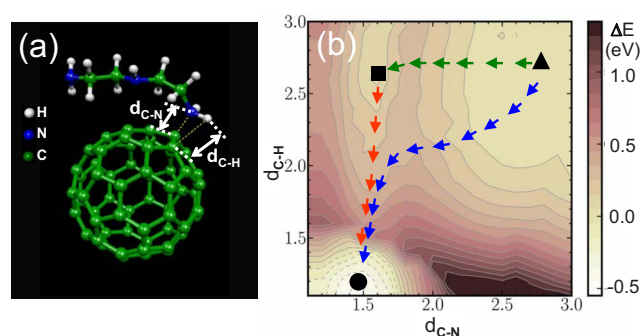


FIG. 3. (Color online) (a) Schematic of the DETA- C_{60} geometry associated with the simultaneous docking and H transfer process, characterized by the key variables d_{C-N} and d_{C-H} . (b) Potential-energy surface of the DETA- C_{60} complex as a function of d_{C-N} and d_{C-H} . \blacktriangle labels the physisorbed state, \blacksquare the docked state, and \bullet labels the final state, with a H atom transferred from DETA to C_{60} .

the temperature necessary to overcome the energy barrier to be $T \approx 200$ K [$E = 0.06$ T kcal/(mol K)], consistent with the experimental observation that polyamines aminate C_{60} at room temperature.²

To better characterize the transition state seen in Fig. 2, we have explored the saddle-point region using the linear synchronous transit (LST) and quadratic synchronous transit (QST) methods as implemented in DMOL3, combined with a standard conjugate gradient optimization of the transition state structure. The transition state has one negative eigenvalue in the Hessian matrix corresponding to an imaginary vibrational frequency of -1581.7 cm^{-1} . Animation of this frequency shows that this mode corresponds to the vibration of the H atom transiting between the terminal N atom of DETA and the closest C atom of the C_{60} cage leading to the energetically favored 1,2-hydroamination adduct.¹⁶ The atomic structure corresponding to the transition state was confirmed by an independent intrinsic reaction coordinate calculation.

To explore the possibility of different reaction paths and to decide if the optimum reaction path is a one-step or a multistep process, we investigated the energetics of the system by varying the values of d_{C-N} and d_{C-H} from 1 to 3 Å by performing 400 independent calculations. The potential-energy surface shown in Fig. 3 represents total energies of the DETA- C_{60} complex that have been optimized with the only constraints being fixed values of d_{C-N} and d_{C-H} . Our results indicate that the transition from the physisorbed state of DETA to the final state of the reaction, where a hydrogen atom has been transferred to the C_{60} cage, may occur either as a single-step process with a slightly higher activation barrier or a two-step process with a lower activation barrier. In particular, the shallow potential well of docked DETA in the d_{C-H} direction suggests an efficient H transfer. Preferred reaction paths are indicated by arrows in Fig. 3.

Careful analysis of our computational results helped us to elucidate the chemical bonding changes associated with hydrogen transfer from DETA to the C_{60} cage. The recently proposed hydrogenation mechanism of C_{60} by polyamines³ suggests the hydrogen transfer to be initiated by an electron transfer from the polyamine to the fullerene followed by a

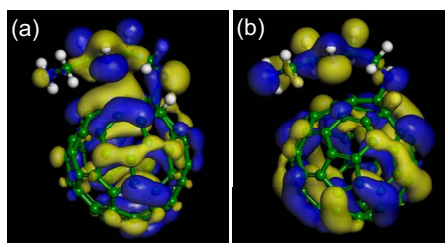


FIG. 4. (Color online) Optimal docking geometry of DETA on C_{60} superimposed with the wave-function isosurface for (a) the HOMO and (b) the HOMO-1. The wave-function phase is distinguished by color.

proton transfer from the N-H group to C_{60} . Close inspection of our results suggests an alternative mechanism, involving neutral hydrogen transfer from DETA to C_{60} during a concerted motion reaction. Both in the previously proposed and the present theoretical scenario, the transfer of hydrogen is promoted by the charge-density lobe near the N atom in the nonbonding highest occupied molecular orbital (HOMO) and second highest occupied molecular orbital (HOMO-1) orbitals of the DETA molecule, depicted in Fig. 4. In either case, the final product is a neutral $C_{60}H$ radical and a neutral N-centered polyamine radical that is missing one hydrogen.

To allow for an independent confirmation of our findings

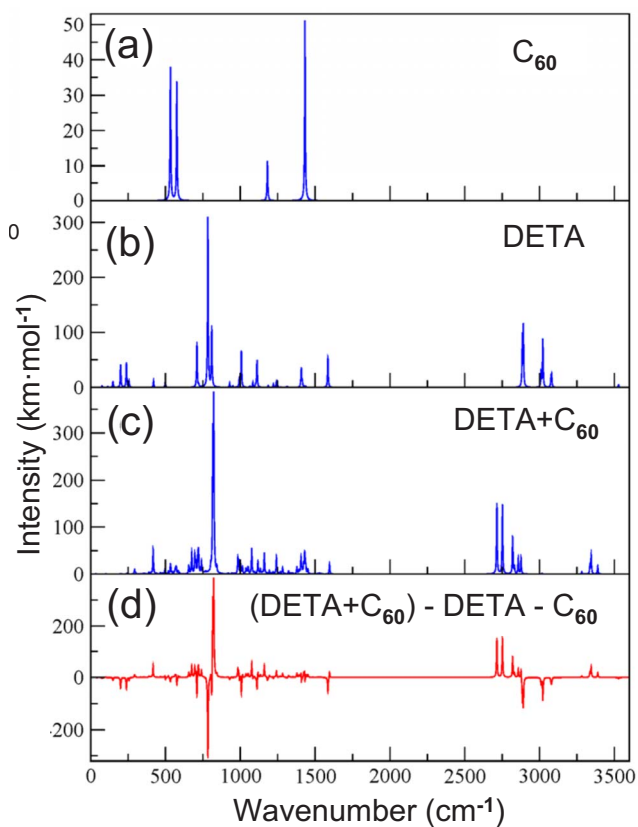


FIG. 5. (Color online) Vibrational frequency spectra of (a) pristine C_{60} , (b) DETA, and (c) DETA docked on C_{60} . (d) The difference spectrum of DETA docked on C_{60} and pristine DETA and C_{60} . The spectra have been convoluted with a Lorentzian function with the full width at half maximum (FWHM) of 5.0 cm^{-1} .

TABLE I. Frequencies of the vibrational normal modes of pristine C_{60} and DETA (in cm^{-1}).

Structure	This work	Expt. ^a	Vibrational mode
C_{60}	531.7	521.0	C-C-C bending
	575.0	571.8	Radial breathing mode
	1180.3	1178.0	Sym. C-C stretching
	1431.4	1424.8	Asym. C-C stretching
DETA	199.9, 238.6		Twisting of terminal NH_2 groups
	419.8		Scissoring of central C-N-C group
	498.8		Scissoring of central N-C-C group
	710.0		Wagging of central H atom
	783.2, 809.0		Wagging of terminal NH_2 groups
	1006.5		Asym. C-C stretching
	1111.5		Asym. stretching of central C-N
	1407.7		Rocking of central H atom
	1585.0		Scissoring of terminal NH_2
	2885.3, 2891.4		Sym. stretching $\alpha\text{C-H}$
	3010.0, 3021.8		Sym. stretching of terminal C-H
	3076.9, 3081.1		Sym. stretching of $\alpha\text{C-H}$
	3528.1		Asym. stretching of terminal N-H

^aReference 18.

regarding the formation of a DETA- C_{60} complex as a necessary prerequisite of the hydrogenation reaction, we performed a vibrational analysis of this adduct, as well as isolated C_{60} and DETA. Calculated frequencies should allow a quantitative comparison with infrared spectra, thus confirming or disproving the presence of the complex. We constructed the Hessian matrix for the final state of the hydrogenation reaction, labeled as ● in Fig. 3(b), using finite differences of the analytical forces with respect to the atomic positions. The normal modes and their frequencies were obtained by diagonalizing the Hessian matrix in mass-weighted Cartesian coordinates. Calculated vibrational frequency spectra of isolated C_{60} and DETA, along with the DETA- C_{60} complex, are shown in Fig. 5. The numerical frequency values along with the normal-mode assignments are listed in Table I. Comparison of our calculated vibrational frequencies with observed spectra for C_{60} in Table I indicates that the theoretical values can be trusted with an uncertainty $\Delta\nu \lesssim 10 \text{ cm}^{-1}$.

In presence of DETA, successful hydrogen transfer to the C_{60} cage cannot be identified by the occurrence of H-related vibrations since both H- C_{60} and DETA exhibit similar H-C stretch modes at frequencies near $\approx 3000 \text{ cm}^{-1}$. Comparison of vibrational modes of the complex in this frequency range, shown in Fig. 5(c), with that of the individual reactants, shown in Figs. 5(a) and 5(b), indicates a frequency shift associated with the coupling between DETA and the C_{60} cage.

The frequency shift can be best judged by considering the difference vibrational spectrum between the complex and isolated DETA and C_{60} adducts. In the complex, we find the band of H-C modes strongly redshifted by $\approx 500\text{ cm}^{-1}$. The coupling between DETA and the C_{60} cage is also reflected in the wagging mode of terminal NH_2 groups of the DETA, which are blueshifted by $20\text{--}30\text{ cm}^{-1}$ due to the stronger coupling between the terminal N and C_{60} in the complex.

So far, we have considered the energetically favorable 1,2-hydroamination adduct as the final state of the reaction. Experimentally, the hydroamination reaction has been reported to lead to $C_{60}H_{18}$, suggesting the docking and subsequent desorption of many DETA radicals on a single C_{60} cage.² If $C_{60}H_{18}$ is the final product, there must be a way to desorb DETA without significantly detaching the chemisorbed hydrogen or modifying the C_{60} cage. In view of the strong bond between the terminal N atom of DETA and the C_{60} cage, we see no simple way to desorb an isolated amine radical. Indirect experimental evidence that this step is not easy may be seen in the fact that DETA chemistry is not gentle, as it requires high temperatures of $205\text{--}380\text{ }^\circ\text{C}$ for successful hydrogenation of C_{60} by polyamines.¹⁷ A possible way to detach polyamines while keeping hydrogen chemisorbed may involve simultaneous adsorption and docking of more than one polyamine at adjacent sites. Following successful hydrogen transfer to the C_{60} cage, the two terminal nitrogens of adjacent DETA radicals could form a covalent

bond while simultaneously desorbing from C_{60} . During this concerted reaction the energy gain associated with the N-N bond formation may be able to offset the energy cost of DETA desorption. In this case, DETA dimers should be observed following a successful hydrogenation.

In conclusion, we used *ab initio* density functional calculations to study the microscopic mechanism underlying the recently demonstrated hydrogenation of C_{60} by diethylenetriamine reagent. Our results indicate that the optimal monoaddition reaction is exothermic, involving an $\approx 0.5\text{ eV}$ high activation barrier associated with the simultaneous docking of the functional group and H transfer to the C_{60} fullerene. We propose to compare our calculated vibrational frequencies with IR spectra to identify the presence of hydroamination adducts, which we propose as a necessary prerequisite for successful hydrogen transfer to C_{60} .

We thank Glen P. Miller for the passionate discussions of the DETA-based hydrogenation of fullerenes. E.K. and P.F.W. acknowledge the support from the U.S. Department of Energy (DOE) under the Grant No. DE-FG36-05GO85028. D.T. and S.B. acknowledge the support by the National Science Foundation under NSF-NSEC Grant No. 425826 and NSF-NIRT Grant No. ECS-0506309. Computational resources were provided by the Michigan State University High Performance Computing Center.

*Present address: Physics and Astronomy Department, Michigan State University, East Lansing, Michigan 48824-2320, USA.

¹G. P. Miller, J. Kintigh, E. Kim, P. F. Weck, S. Berber, and D. Tománek, *J. Am. Chem. Soc.* **130**, 2296 (2008).

²J. B. Briggs, M. Montgomery, L. L. Silva, and G. P. Miller, *Org. Lett.* **7**, 5553 (2005).

³J. Kintigh, J. B. Briggs, K. Letourneau, and G. P. Miller, *J. Mater. Chem.* **17**, 4647 (2007).

⁴K. L. Lu, R. M. Lago, Y. K. Chen, M. L. H. Green, P. J. F. Harris, and S. C. Tsang, *Carbon* **34**, 814 (1996).

⁵A. Koshio, M. Yudasaka, and S. Iijima, *Chem. Phys. Lett.* **341**, 461 (2001).

⁶B. Delley, *J. Chem. Phys.* **92**, 508 (1990).

⁷B. Delley, *Phys. Rev. B* **66**, 155125 (2002).

⁸J. M. Soler, E. Artacho, J. D. Gale, A. García, J. Junquera, P. Ordejón, and D. Sánchez-Portal, *J. Phys.: Condens. Matter* **14**, 2745 (2002).

⁹J. P. Perdew and Y. Wang, *Phys. Rev. B* **45**, 13244 (1992).

¹⁰W. J. Hehre, L. Radom, P. R. Schleyer, and J. A. Pople, *Ab Initio Molecular Orbital Theory* (Wiley, New York, 1986).

¹¹J. Junquera, O. Paz, D. Sánchez-Portal, and E. Artacho, *Phys. Rev. B* **64**, 235111 (2001).

¹²J. P. Perdew and A. Zunger, *Phys. Rev. B* **23**, 5048 (1981).

¹³N. Troullier and J. L. Martins, *Phys. Rev. B* **43**, 1993 (1991).

¹⁴L. Kleinman and D. M. Bylander, *Phys. Rev. Lett.* **48**, 1425 (1982).

¹⁵R. I. Masel, *Principles of Adsorption and Reaction on Solid Surfaces* (Wiley, New York, 1996).

¹⁶In our context, the chemical notation “1,2-hydroamination adduct” means that the DETA amine radical and the transferred H atom are chemisorbed on neighboring C atoms of C_{60} .

¹⁷Glen P. Miller (private communication).

¹⁸S. Pandi and D. Jayaraman, *Mater. Chem. Phys.* **71**, 314 (2001).